Presented at IPC Printed Circuits Expo®
SMEMA Council APEX®
Designers Summit 04

Mechanical Bending Technique for Determining CSP Design and Assembly Weaknesses

Mark R. Larsen, Ian R. Harvey Ph.D.,
University of Utah
Salt Lake City, Utah

David Turner
Inovar, Inc.
Logan, UT

Brent Porter
Bourns Electronics
Cork Ireland

Jm Ortowski
EDO Ceramics
Salt Lake City, UT

Abstract
A cyclic board-bending technique has been developed to ensure a reproducible multiaxial stress state at the Chip Size Package (CSP) solder fillet. Mechanically stressing the package serves as a valuable tool to quickly determine and provide feedback on design and assembly weaknesses, 20-30 times faster than less comprehensive data can be obtained using temperature cycling.

The bending technique allows controlled strain application rate, peak strain, and dwell time as experienced by a population of ten components per each of ten board positions. Board surface strain for each of these positions is characterized using strain gages. The plastic, transition, and elastic regions of the PCB are determined experimentally according to peak strain and correlated with failure mechanism. Two main failure modes are made manifest through Weibull techniques: board-level failures (plastic board response region), and solder joint failures (elastic board response region). Cyclic bending results compare different CSP architectures thus demonstrating the utility of the test technique.

Key words
PCB, cyclic bend testing, chip scale package, CSP, solder joint reliability, fatigue cracking, board flex sensitivity, tensile stress, surface mount, and delamination.

Introduction and Background
Results previously published by this group[1] looked for architectural and silicon thickness effects on reliability performance, as measured by a novel board-bending technique. Temp cycling was effective in demonstrating differences in experimental parameters[2], but bend tests were confounded by the fact that elements within the board (i.e. copper runner, pad interface) fatigued and failed faster than component solder fillets. The CSP failure trends were independent of designed experimental variables. All components were deemed ‘equivalently’ robust to bending by virtue of having outlasted the board upon which they were mounted.

Figure 1 indicates the overall bending data summary from the earlier test, with differing silicon thickness and ball attach approaches[1]. Three silicon thickness splits were used for both the “wide via” and “narrow via” architectures. The chip thicknesses of 200, 300, and 400 microns, were achieved by atmospheric downstream plasma[3]. The “tails” in the previously reported Weibull plots were attributed to the then uncharacterized stress states from row position 1 to row 10.

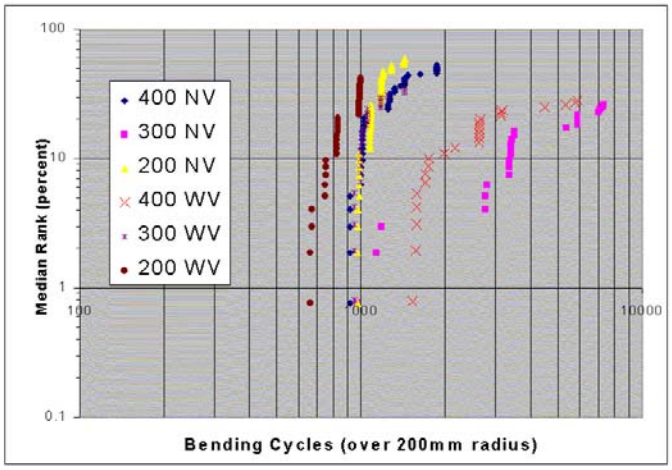

Figure 1 - 4x5 daisy chains / 0.5mm pitch / 0.3mm Solder Ball / 0.8mm Multilayer Board with Surface Routing under Cyclic Bending in the 5x Direction - Six Experimental Splits Covering Silicon Thickness (Microns) and Solder Ball Attach Architecture (Wide Via vs. Narrow Via) are Indicated[1]. - Bending Data are Confounded by a Failure Mechanism which is Independent of the Experimental Variables: Board Level Fatigue

It was anticipated that cyclic bend testing conditions, which maintain shear stress strictly in the elastic board response region, would yield a fillet failure. When the board responds elastically only, the stresses caused by bending should be localized to the solder joint between the silicon and PCB, and the stress transmitted across the fillet should be consistent with every cycle.

This paper explores possible reasons for the variable board failure observed previously, by reporting empirical characterization of stress states and the correlation with failure mode.

Experimental Approach

More boards, like those used in collecting data for Figure 1 (0.8mm thick, 6-layer HDI, Ni/Au finish), were assembled and stressed to 5 million cycles in order to capture the elastic/plastic board response transition. Sample devices were from two populations representative of wide via (passivation directly supports a rigid attachment of the UBM film) and narrow via (a BCB layer buffers the space between passivation and UBM, with a relatively small ohmic contact – or via – between the I/O pad and the UBM). Torsional stress at the board runner was reduced by rotating the boards to stress in the 4x direction of the chip I/O array, rather than the 5x direction used previously. (0.5mm pitch daisy chain CSP in 4x5 I/O array, being bent in the 5x direction.)

The fixture for bend testing as designed and built at Bourns uses a 200mm radius of curvature and operates at 1 Hz (Figure 2). One edge of the board is clamped and the opposite edge is then forced downward over the radius creating a reproducible family of stress states with every cycle. The stress-state depends upon the position of the DUT relative to the clamp.

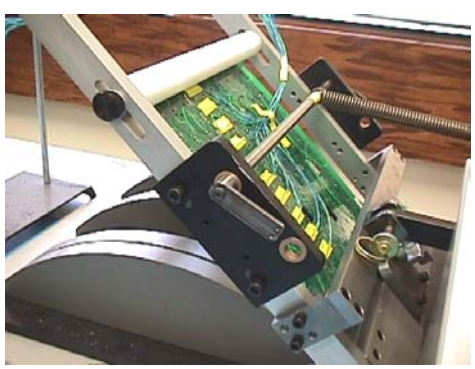

Figure 2 - Board-Bending Apparatus with 200mm Radius of Curvature Operates at 1 Hz. 100 Daisy Chain Parts are Tested Simultaneously - 10 Parts per Row Constitute a Population with a Given Imposed Strain Energy State - Wires seen coming off the Board are attached to Strain Gages associated with each Row Position

Testing takes advantage of daisy-chain circuitry to increase the sampling size. Continuous monitoring uses a Keithley 2400 "digital source meter". A threshold resistance of 10x the baseline daisy chain resistance is set (sourcing 100uA). When the threshold is superceded, the Keithley trips a relay and stops the rack in the unstressed position.

Prior to bend testing, isoelastic strain gages (JP Technologies Inc., model PINC-250BA, 1000 ohms, 3.228 gage factor) were mounted directly to the PCB and aligned with all ten rows of parts. A data collection program was written to simultaneously collect strain gage resistance as seen by three digital multimeters. The DMM's were set to capture one thousand measurements in a one-second cycle. A data reduction program subtracts line noise and tabulates the strain to produce graphs for each device position. This enabled the generation of strain data demonstrating the presence of a strain shock event as discussed below.

Experimental Learning Curve

Understanding the design and configuration of the bending apparatus, it was anticipated to see the first failures on the clamped end of the board, and then gradually decrease toward the roller end of the board. However, when the failures from the population were tabulated on a per-row basis (see Figure 3), an anomaly was observed.

Analysis of the failure data indicates a useful profile to failure occurrence at each row of the board during bend cycling, and gives a relative indication of the types of stresses responsible for creating these failures. The board failure rate is observed to peak at row 3, then manifest the anomalous high failure peak at row 8. (A smooth rate falloff from the clamp side to the roller side of the board was expected.)

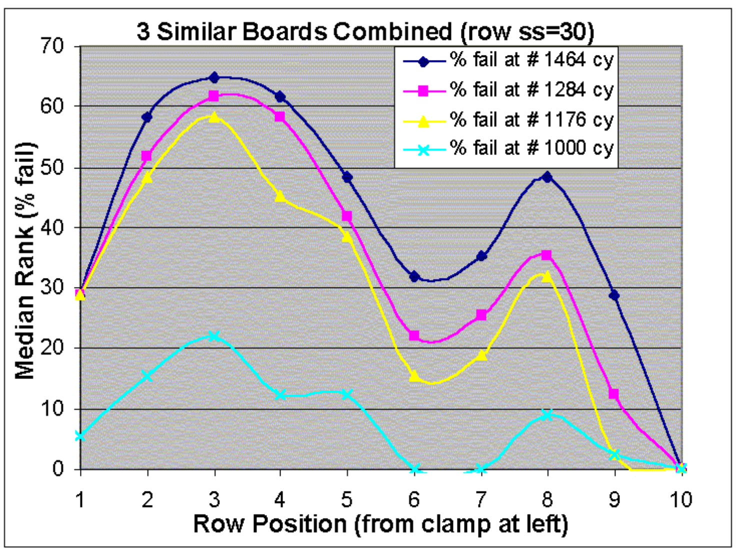

Figure 3 - Failure Trends during Previous Testing (Data on Similar Boards taken from Figure 1)
Note the profile with peaks at rows 3 and 8. Note also that row 10 has not been stressed to the point of failure, even with the other anomalous stress peaks.

Push-Down Control

The original design of the testing fixture used two pair of steel rollers (see Figure 4a) to assist in forcing the board over the radius. (All previously published testing was done with this push-down control in place.)

With the implementation of strain gages in the most recent testing, results showed that the rollers were causing a significant strain shock at the board level. Some evaluation was performed with the push-down control removed and it proved unnecessary to implement it further. Thus, all further data were collected with the rollers removed as in Figure 4b.

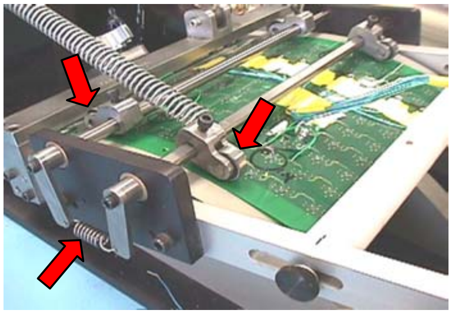

(a)

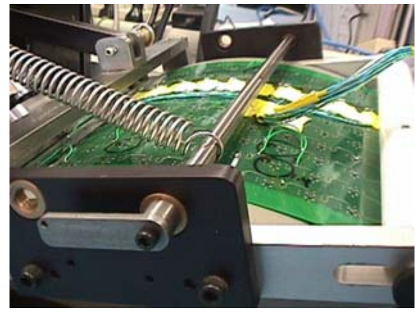

(b)

Figure 4 - (a) Bend Testing Apparatus with the Spring-Tensioned Rollers in Place; and (b) with the Rollers Removed

Note in (b) that the board wraps uniformly about the set radius despite the absence of the "push-down" system.

Family of Strain Conditions

Figure 5a shows the strain shock profile caused by having the push-down control implemented (per Figure 4a). Figure 5b shows the improvement when the push-down control is removed. Note that there is no significant change in peak strain for the first five rows, but the board level shock has been eliminated and the peak strain actually increases for subsequent rows. *This observation is important to indicate the role played by strain application rate (impact shock) in accelerating failure*.

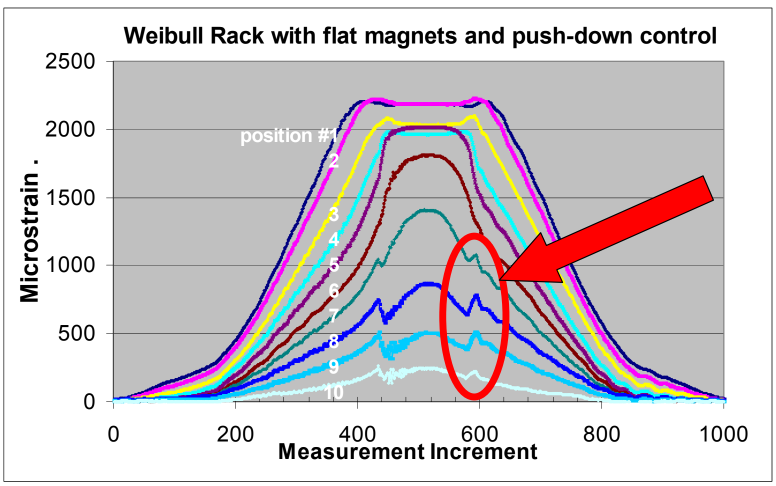

(a)

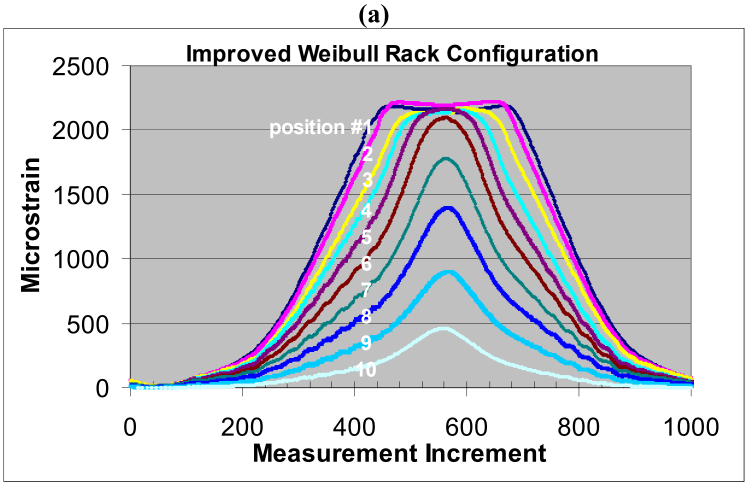

(b)

Figure 5 - Strain Profiles for each Position of the Board, Relative to the Clamp - Initial Profiles (a)Using the Push-Down System as shown in Figure 4a, and Improved (b) Apparatus Configuration

Note in (a) the indications of strain shock.

Periodic measurements were made during life testing to observe that drifting effects were minimal and there were no significant changes in peak shape or maximum strain over time.

Failure Performance

Figure 6 shows how the tendency to fail generally tracks with position in a manner more consistent with expectations, with the improved tester configuration as compared to Figure 3. Note that the anomalous failures at row 8 have been eliminated. All current results implement the 4x5 daisy chain with bending done in the 4x direction, rather than in the 5x direction as reported previously[1], so relative trends are more significant than absolute cycle life magnitude.

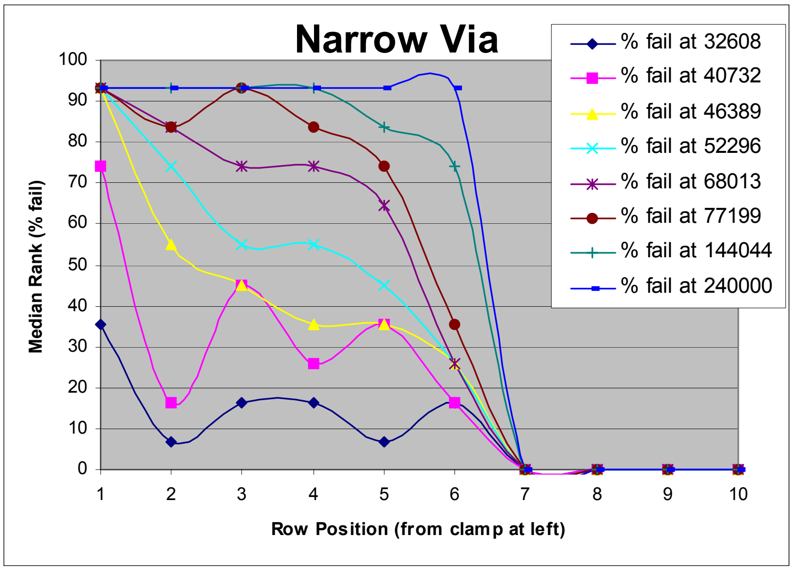

Figure 6 - Tracking of Percent Failure Up to 240,000 Cycles on the Improved-Configuration Bend Tester - At this Point there are No Failures on Rows 7 through 10, and Rows 1 through 6 indicate a Common Failure Characteristic

The first six rows fail at close to the same rate, suggestive that peak strain is the more dominant of the two factors shown in Figure 7. Rows 1-6 are thus grouped together as a common population for use in Figure 8. This plot is suggestive that the failure mechanisms present in the first six rows are different than those present in row 8, while row 7 is expected to be transitionary[4].

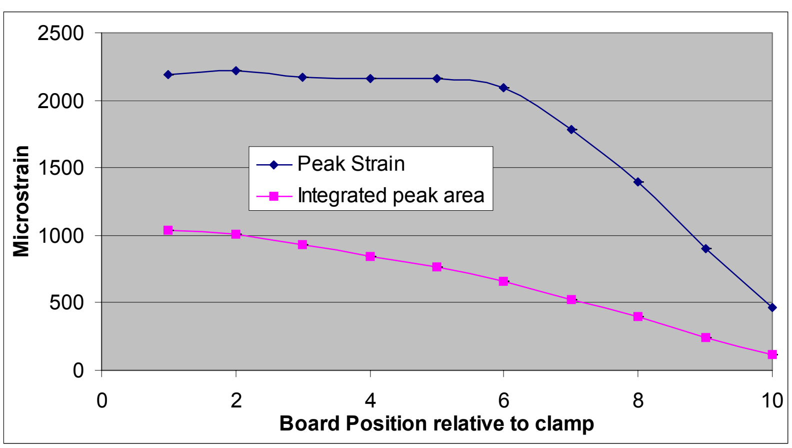

Figure 7 - Plot of Peak Strain (Upper Data Set) and Relative Integrated Strain Area (Lower Data Set, Relative Values) for Each

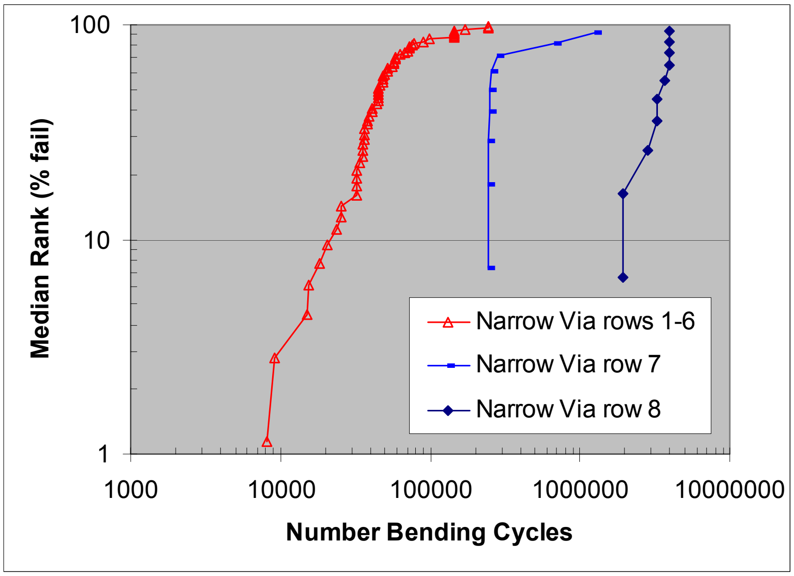

Figure 8 - Weibull Plot of Grouped Rows 1 through 6, and Single Rows 7 and 8, as Generated from the Mechanical Bending System - Changing Slopes of the Failure Curves for the Different Board Positions indicate Possible Changing Failure Mechanisms for Varying Board Position Stress States

A second copy of the Weibull Rack was built. This rack was characterized and configured to produce a strain family as close as possible to the first test system. So-called "Weibull Jr." ran an identical board assembled with 400 micron silicon, in ball attach architecture using the wide via (UBM directly attached to passivation). The results comparing wide via performance with narrow via are shown in Figure 9. This plot suggests that transitionary behavior is still being manifest by the row-8 devices on the wide via board. The test was discontinued prior to the onset of failure in row-9 for either of the boards.

The sandwiched BCB in the narrow via structure may add sufficient compliance to create the observed difference in fatigue performance.

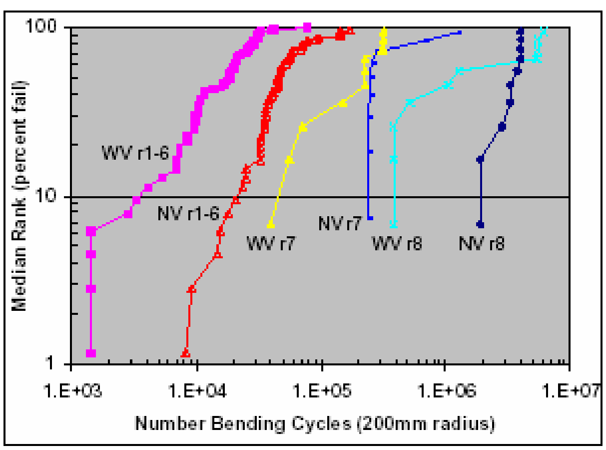

Figure 9 – Narrow via Architecture Demonstrates Consistent Superior Bending Fatigue Resilience Due to the Compliant "Cushioning" Effect of the BCB under the Bump

Correlation to Failure Mechanism

Multiple cross-sections were taken at each position on the narrow via and wide via boards after the entire population on rows 1 through 8 had failed (no failures on rows 9 and 10) when testing was aborted at 5 million cycles.

There was no significant difference in failure mechanism between wide via and narrow via splits in the tests, so above results from narrow via parts are used as being representative.

Figures 10 and 11 shows the type of failure that can occur as the surface runners break and create an open. This is the same mechanism reported earlier with respect to the data of Figure 1, and represents the "plastic" strain response at the board level. Figure 11 also shows the common problem of the solder ball being ripped off of the pad. Figure 12 shows the Si/UBM side of the same fillet where a crack is propagating through the solder. In this case, repeated loading has caused a fatigue crack to propagate along the intermetallic interface with the solder fillet near the UBM side. The initiation site for this crack is at the inboard side of the solder fillet, common for all cross-sections evaluated in this test.

Note the significant difference in this mechanism, relative to TC-fatigue arrays, whose cracks initiate on the outboard side of the bump. Coarsening through the solder fillet is also substantially less for bend tested microstructures than typically seen in parts from temperature cycling tests.

Multiple cross-sections cut from the boards at 10k-15k cycles confirmed that all three mechanisms were active simultaneously on rows 1-6.

After millions of cycles (row 7 and beyond), the ultimate cause of failure was difficult to discern between the pad-level transverse fillet failure and the near-UBM fillet failure, since both active mechanisms were capable of causing open circuits. Devices taken from rows 9 and 10 (no failure yet) also indicated the beginning of the two active fillet mechanisms, but showed no board runner fatigue.

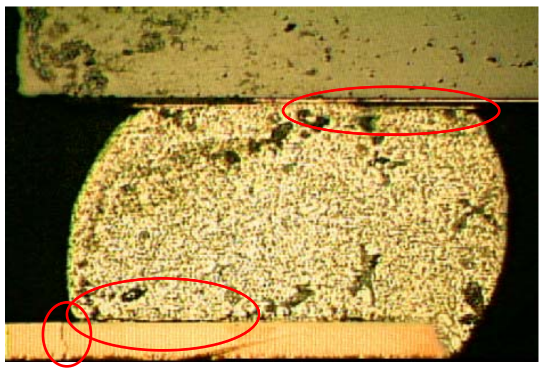

Figure 10 - Typical (*Narrow Via*) Solder Fillet as Found on any Row 1-6 Device Edge - Three Crack Mechanisms were Active Simultaneously on Rows 1-6
Note vertical runner crack just at the left of the solder mask-defined fillet edge. There is a crack at the pad surface that runs along the intermetallic layer, and there is a crack that starts at the inboard side of the fillet near the UBM and runs through the solder to the outboard side. The runner failure is absent beyond row 7.

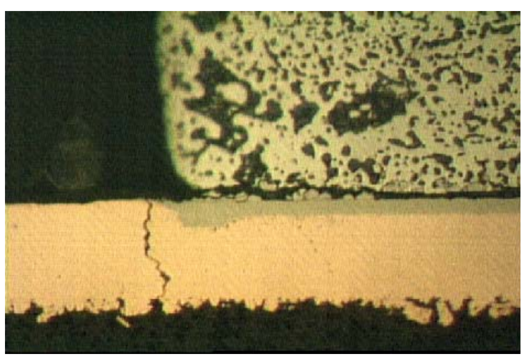

Figure 11 - Magnification of Lower Left Corner of Figure 10 - Strain was so Great on the Board at this Part, that not only did it Pull the Solder Ball Off of the Pad, but it also caused a Tear in the Surface Runner - This Image is Typical of all Parts in Rows 1-6 and some in Row 7 - No Runner Cracks were Observed in the Samples Taken Beyond Row 7.

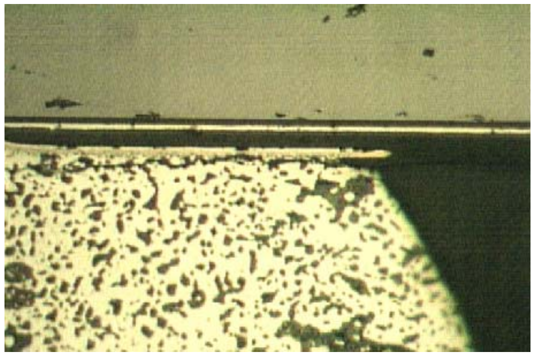

Figure 12 - Magnification of Upper Right Corner of Figure 10; Fatigue Crack Propagating through the Interface of the Solder and Under Bump Metal - This Type of Failure Mechanism is in a Similar Location to those Found when Placing the CSP Parts into Temperature Cycling, but Initiates on the Inboard Side of the Bump and Works its Way towards the Chip Perimeter

Discussion

Failure trends were compared with strain gage data for each board position to approximate a strain range at which there is a transition from the board level fatigue, to exclusively solder-level fatigue. Table 1 lists the different failure mechanisms caused by the board-bending test.

Table 1 - Breakdown of the Three Failure Mechanisms Present

Microstrain range	**Description**	**Example** (rows seen)
>1500	Breaking of board runners	Fig. 12 (rows 1-7)
all	Pulling solder ball off of pad	Fig. 12 (rows 1-8)
all	Fatigue crack at or near UBM	Fig. 13 (rows 1-8)

New Configuration Results

Strain gage characterization resulted in optimization of a very reproducible and versatile testing system: multiple failure mechanisms can be studied with reasonable statistical significance in one test. Harsh, multiaxial stress conditions which cause board-level failures, more mild conditions resulting in solder joint fatigue, as well as those that fall in transition, can all be studied and evaluated during a single quick test.

Comments on Failure Mechanism

Whereas TC cracks typically occur during the cooling cycle and initiate on the outboard side of the bump, yet during bending the crack is initiated on the inboard side of the fillet nearest silicon and propagates toward the outside of the chip. This failure mechanism is more subtle than TC fails, because (1) domain coarsening receives no thermal activation as in TC tests and is therefore not manifest near the crack, and (2) the crack surfaces do not abrade one another during cycling (rather open and close), so are not as readily visible. However, recent published evaluations[5] of a cell phone (CSP mounted opposite to the keypad) used in the field indicate that bending fatigue cracks exhibit the patterns of elastic bending as seen beyond row 8 in this study.

Field Fatigue Mechanism

An Ericsson T39 cell phone was subjected to normal field use for approximately one year, then taken apart for evaluation[5]. It has been stated in this study that row 8 appears to be exclusively within an elastic board response strain level, such that every cycle generates an identical low-load stress transmitted across the fillet. It is this condition that mimics the actual application environment as correlated to the cracking characteristics of the device stressed normally in the field. The correlation is exact, down to the interior location of crack initiation sites, and lack of domain coarsening common to thermal fatigue.

Bend Testing Apparatus Summary Observations

- The mechanical bend testing apparatus is designed to provide rapid feedback to process engineering as to presence of any process or architectural weakness.
- Time to data is typically 2-3 days per board (worst-case plastic response) plus failure analysis.

- TC takes ~20-30x longer to collect comparable data, based on number cycles to fail on comparable boards, assuming fillet wearout in both cases.
- Unlike temperature cycling, the bending apparatus offers simultaneous, reproducible shear plus tensile stress combination states.
- Mechanical bending can be used in conjunction with temperature cycling to precondition boards prior to temperature cycling test.
- Rapid qualification of a CSP/board/ass'y *system* is possible.
- Relative CSP robustness is compared to board life for qualification purposes.
- Large sample sizes in bending enable Weibull analysis and give confidence to results.
- Multiple stress states in a single test provide for characterization of board-level contributions to overall reliability.
- Worst-case bending is designed to catch latent weaknesses.
- Lower strain states more closely correspond to typical handheld electronic applications.

Conclusions

While prior test results were effective in conclusively determining the robustness of a set of CSP components; those results were unsatisfactory in correlating planned experimental variables with bending or temperature cycle reliability. Test system improvements have been presented that can enable comparison of different design and assembly attributes under diverse strain conditions. In the case of the two boards presented here, both performed at maximum effectiveness, and no difference was discernable between them.

Important factors in driving failure mechanisms are considered to be (1) peak strain, (2) strain application rate (shock events), and somewhat less influential is (3) strain hold, or strain energy imparted within a given cycle.

For this board style (0.8mm, 6 layer surface routed, Ni/Au finish), the elastic response lies below approximately 1500 microstrain, as measured in surface shear. Other board styles would need to be separately characterized.

Bend testing comprehends a worst-case combination of tension and shear in a reproducible test, and overtly offers the comparison relative to the board. TC is almost exclusively shear in nature, and therefore fails to activate process or architecture weaknesses, for example, that are related to weak interfacial adhesion. TC performance dependencies are also more subtly dependent upon board characteristics, and it is more difficult to separate board (e.g. thickness) effects for cross-platform comparison.

Future Work

Use of optimum board pad design (microvia-in-pad) under which a fillet failure can be reproducibly generated.

Use of an electrodynamic transducer system to drive a four-rod bend configuration at 5 Hz, 1000-1500 microstrain (sinusoid) to rapidly simulate low (elastic) load, high cycle strain conditions, and simulating the routine use of a cell phone.

Acknowledgments

Testers, boards, parts, tooling, and development funded by Bourns Electronics, Logan, Utah.

This work is a combined effort of multiple individuals of the Bourns Thin Film group: Chris Herbert, Ian Doyle, Jim Somers, William Flynn, and Barry Sheehan. Support from the Bourns/Logan tooling group is appreciated: Jeff Buttler, Bob Grutzmacher, Craig Smith, Nick Hawker, Mike Dickman, Shane Leishman, Hans Parkin, and Zan Aslett. The bumping expertise at Flip Chip Technologies is appreciated, including DH Kim, Pete Elenius, and Scott Barrett. Bourns acknowledges the board manufacturing of JVC and contract manufacturing of Nextek, Inc. Wafer-level thinning was courtesy of Pat Halahan of Tru-Si technologies.

References

1. I.R. Harvey, J. Ortowski, D. Turner, C Herber, "Empirical Strategy for Characterizing and Minimizing Effects of Flexure-Induced Tensile Stress in CSP's", IMAPS-IJMEP, vol 23, num 4, 4th quarter 2000
2. I.R. Harvey, J. Ortowski, D. Turner, C. Herbert, "Optimization Case Study of CSP Temperature Cycle and Board Bending Reliability", APEX 2001, Jan. 16-18, San Diego, CA (to be published)
3. Savastiouk, S., Siniaguine, O., Hammond, M., "Atmospheric Downstream Plasma - a new tool for semiconductor processing", Solid State Technology, June, 1998.

4. K. Jonnalagadda, “Via-in-pad Reliability in Mechanical Cycling Fatigue”; Proc. 2000 International Symposium on Microelectronics, Sept. 20-22 Boston, MA
5. I.R. Harvey, M.R. Larsen, J. Somers, I. Doyle, “Correlation of CSP Bending Fatigue in a Cell Phone to a Unique Predictive Cyclic Bending Test”, IEEE/EDS workshop, Boise ID, 25 October, 2002

MECHANICAL BENDING TECHNIQUE FOR DETERMINING CSP DESIGN AND ASSEMBLY WEAKNESSES

Mark R. Larsen

Graduate Student

February 26, 2004

IPC TECHNICAL CONFERENCE
PRINTED CIRCUITS EXPO®
SMEMA COUNCIL APEX®
DESIGNERS SUMMIT

San Anaheim, California

February 24-26, 2004

Basis of Work

- **The work that is outlined in this presentation was done while at Bourns**
- **Much of the information collected and published was a combined effort of the following individuals:**

Mark R. Larsen, Ian R. Harvey, Ph.D.

University of Utah

Salt Lake City, Utah

David Turner
Inovar, Inc.
Logan, Utah

Brent Porter
Bourns Electronics
Logan, Utah

Jim Ortowski
EDO Ceramics
Salt Lake City, Utah

Order of Presentation

- Temperature cycling performance
- Cyclic board bending approach and results
- Relationship to field use devices
  - Compared to temperature cycling
  - Compared to bend cycling
- Future work
- Summary, Conclusions, and Questions

Field → Empirical → Predictive Simulation

-40 to 125 ºC / 15 min ramp / dwell

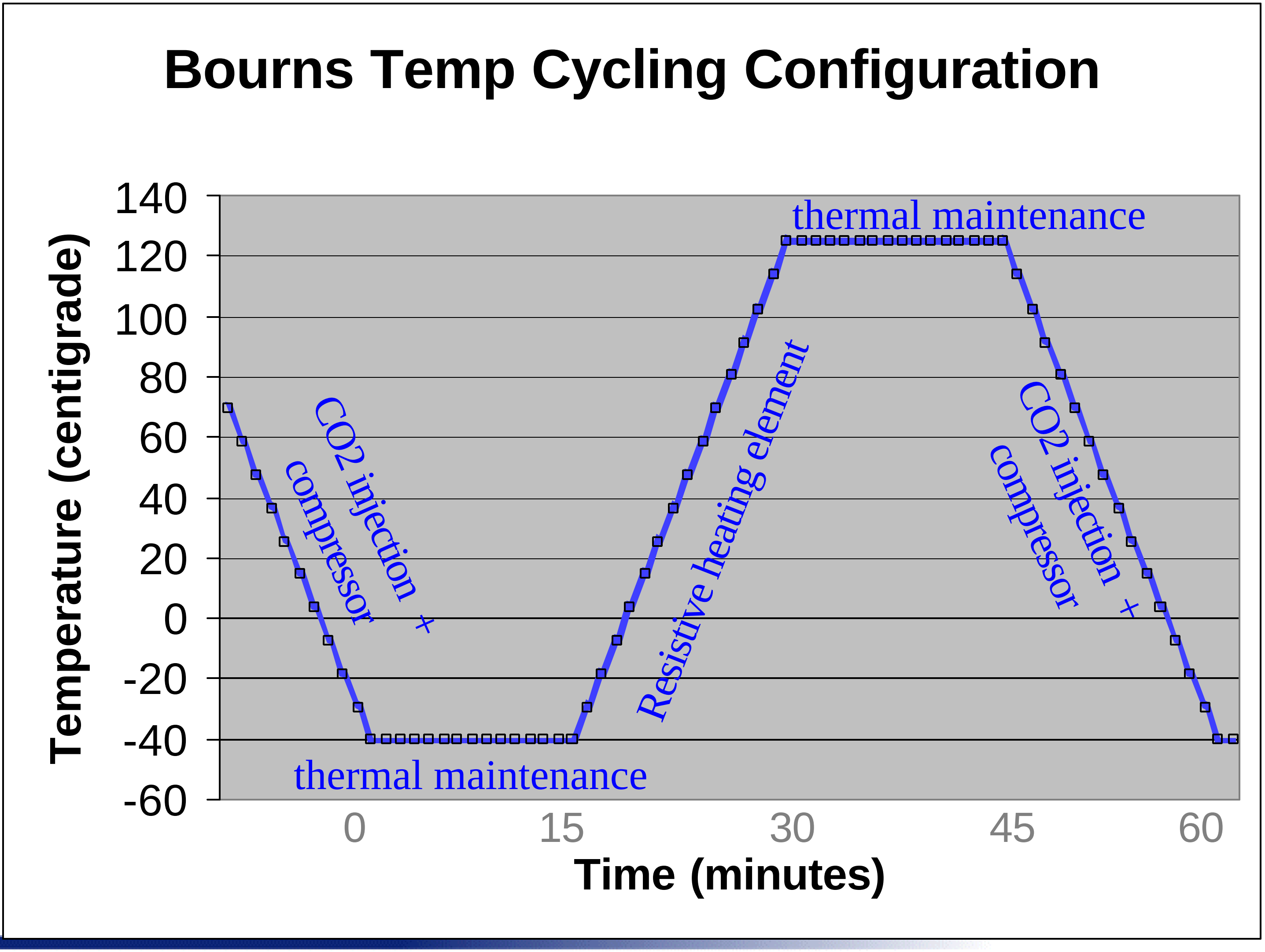

Temperature Cycling Results

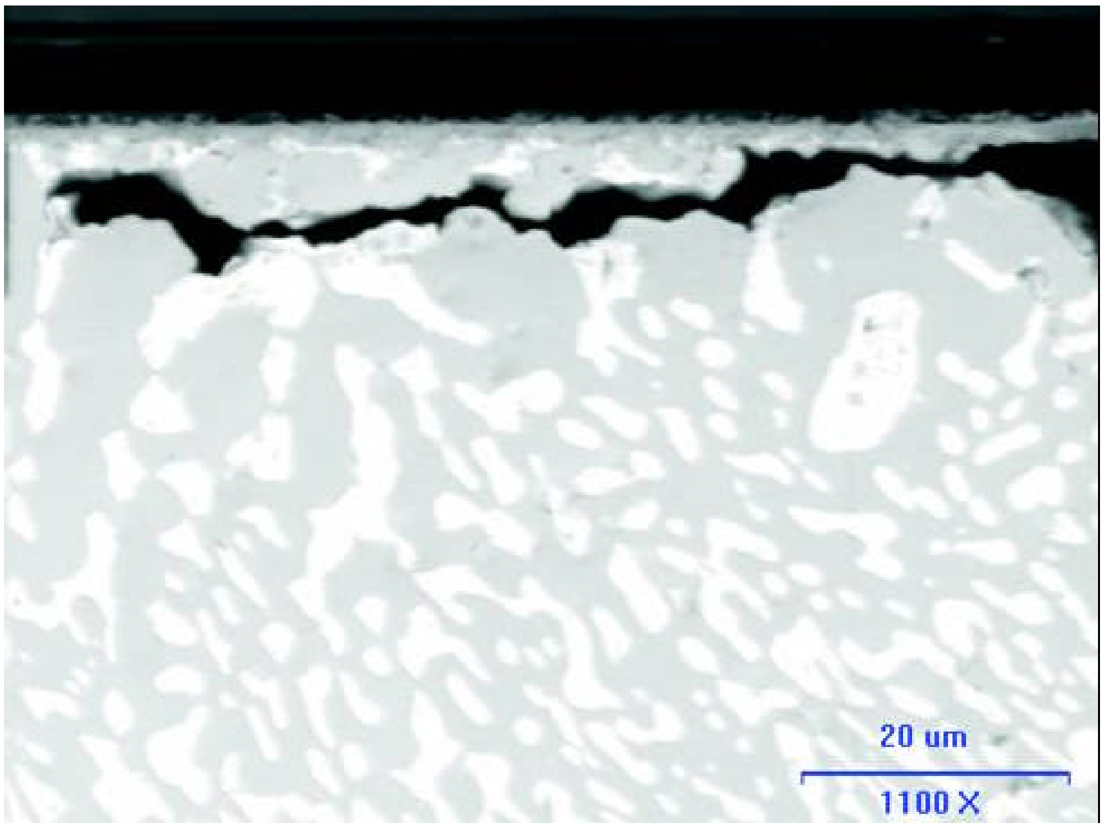

- Coarsening of the primary lead / tin domains
- Crack propagation through solder bump near silicon
- Crack begins at “outer” edge and works in

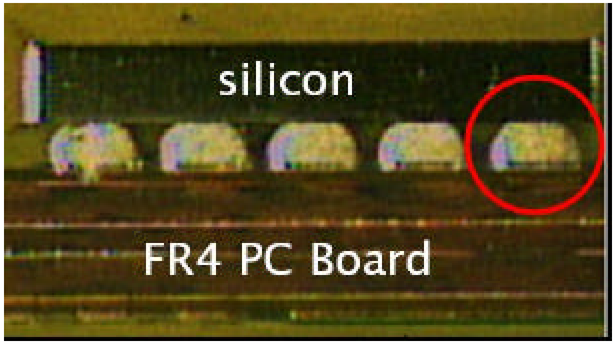

First Generation Manual Bend Test Fixture

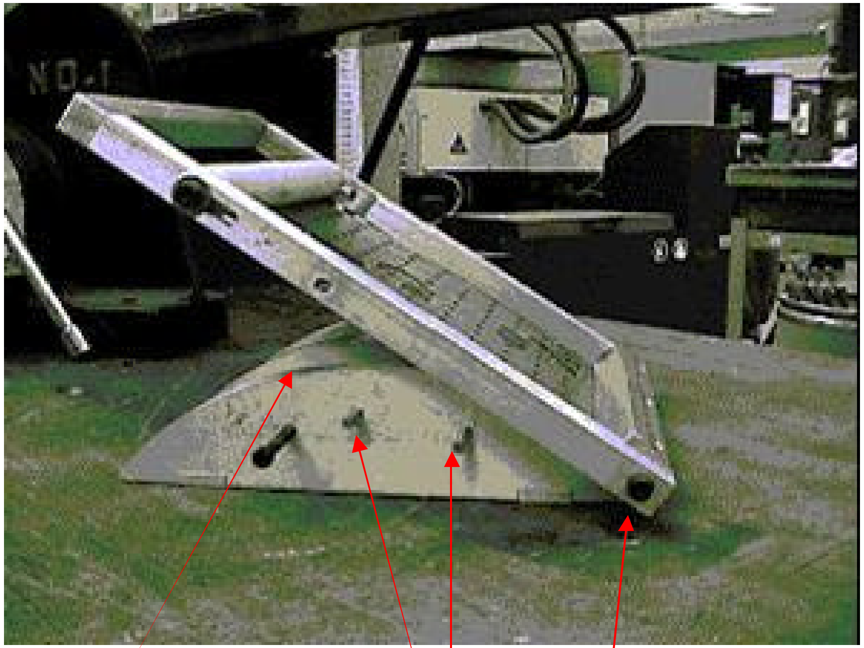

Cyclic Bend Test Fixture

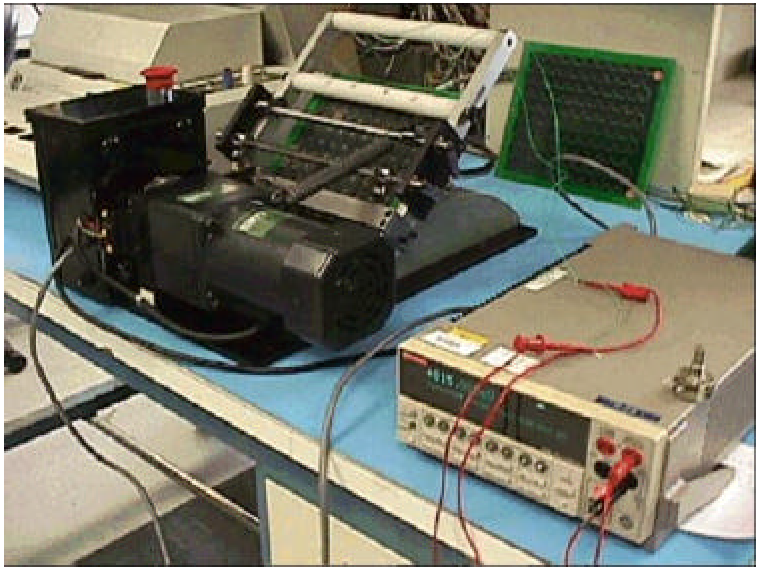

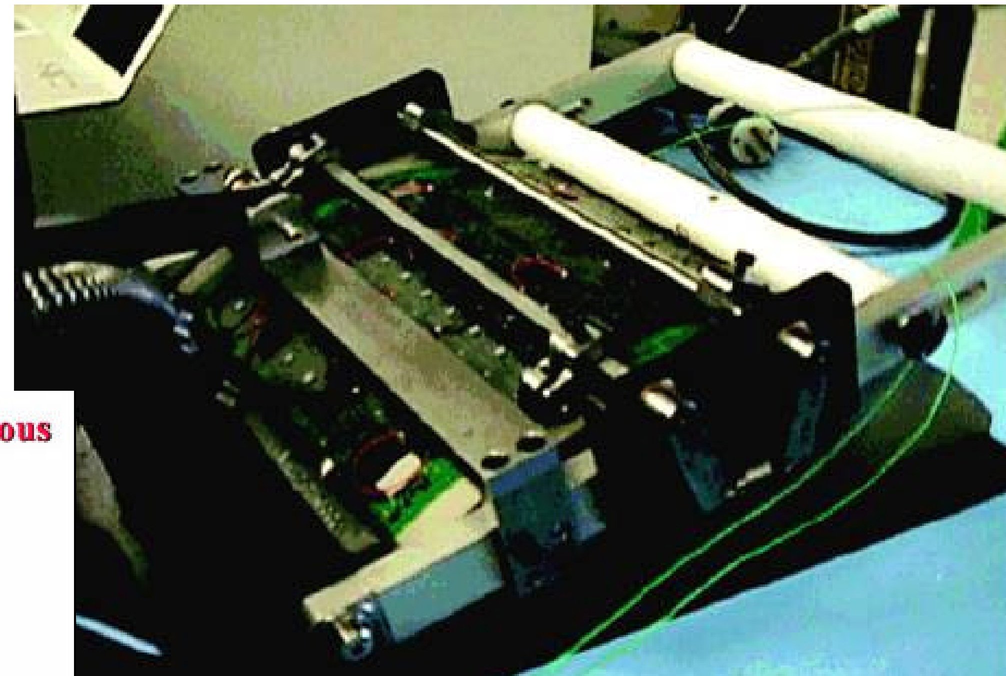

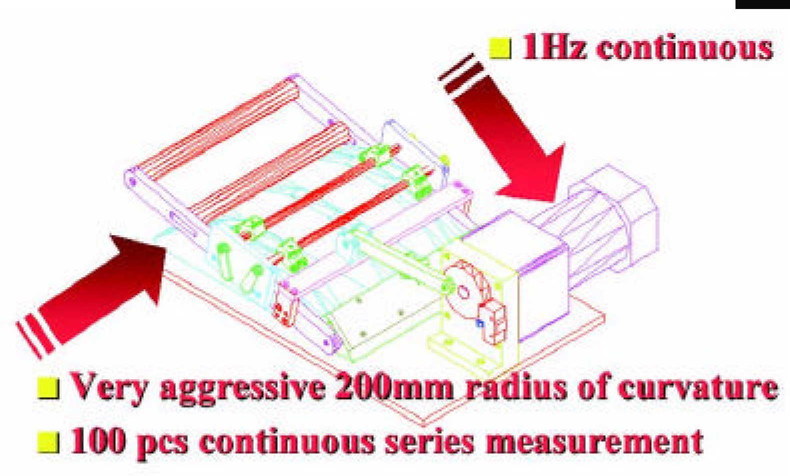

First Impressions

- Problem
  - Drastic failures
    - Ripping solder bumps away from pads
    - Loosing electrical contact after breaking board runners
- Solution
  - Implement strain gages for microstrain readings
  - Correlate strain gage data to failure data

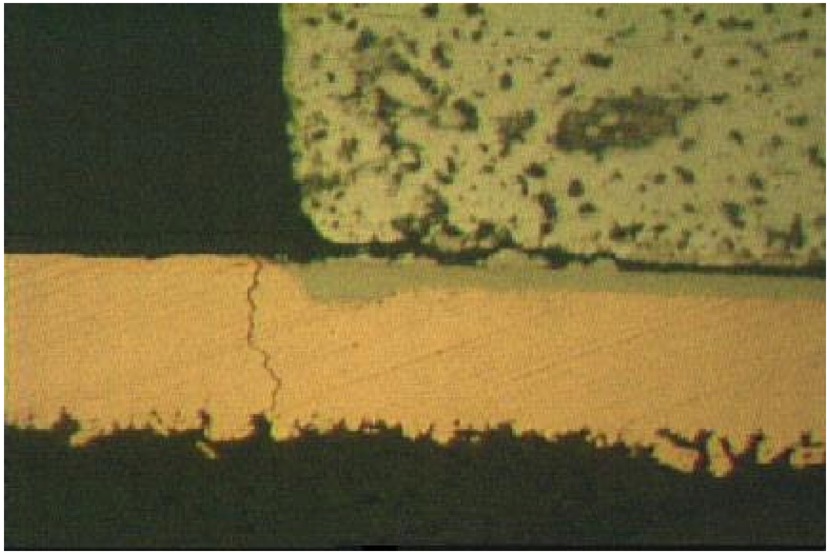

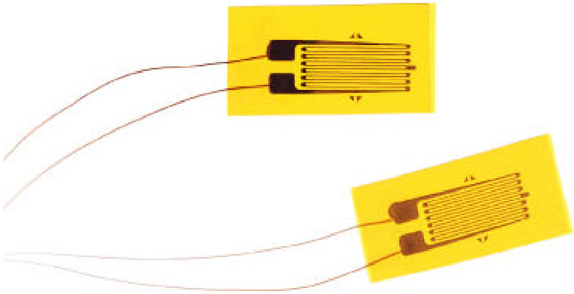

Characterization of Board Strain

Rows 1 – 10 Each Evaluated Individually

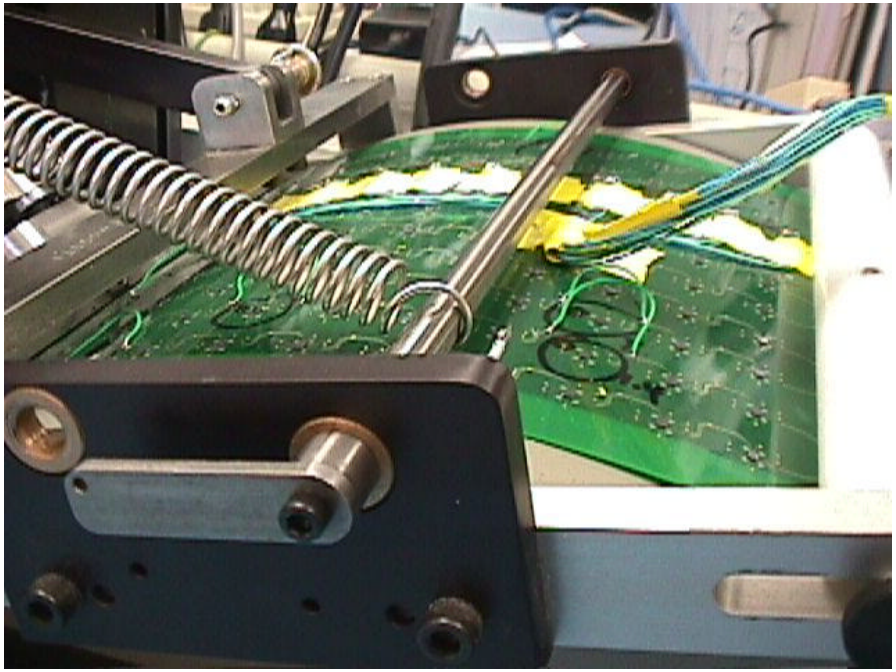

-- Relax the throw slightly…

Strain Gage Data vs. Failure Data

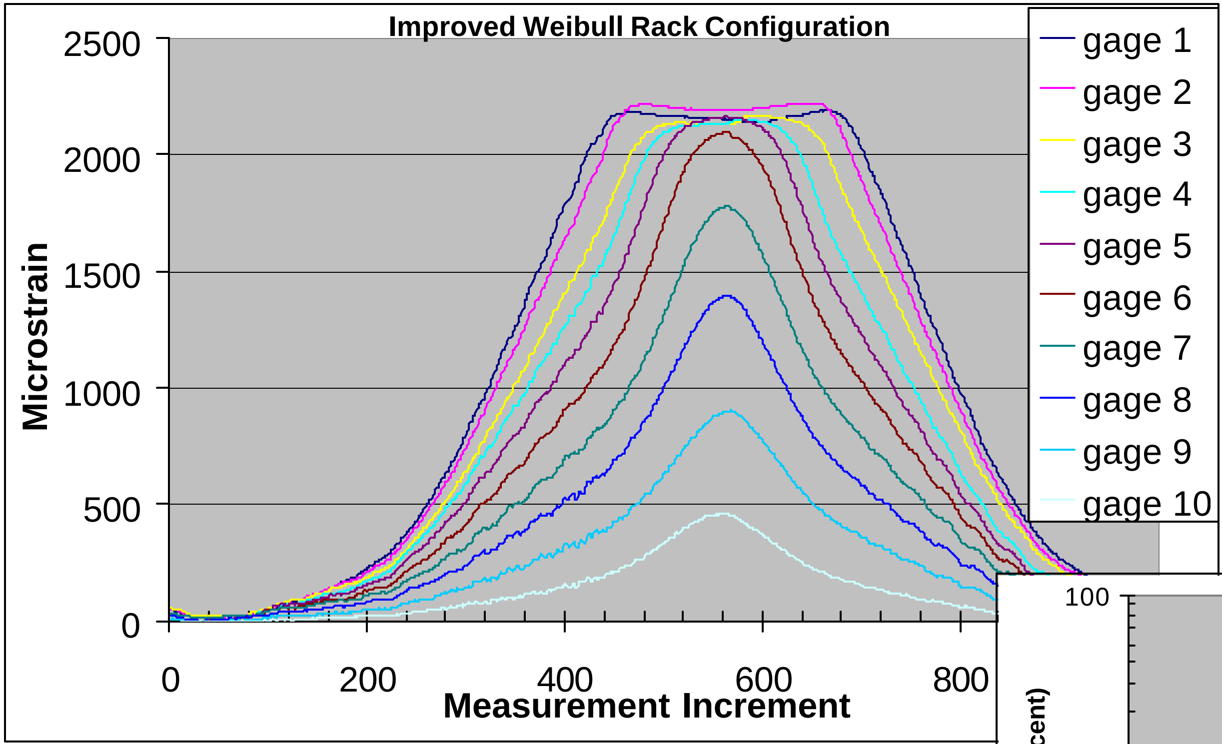

Gage number correlates to board position (or row)

- **“Plastic” board response**
  - **Rows 1 - 6**
- **Transitional response**
  - **Row 7**
- **Elastic board response**
  - **Rows 8 - 10**

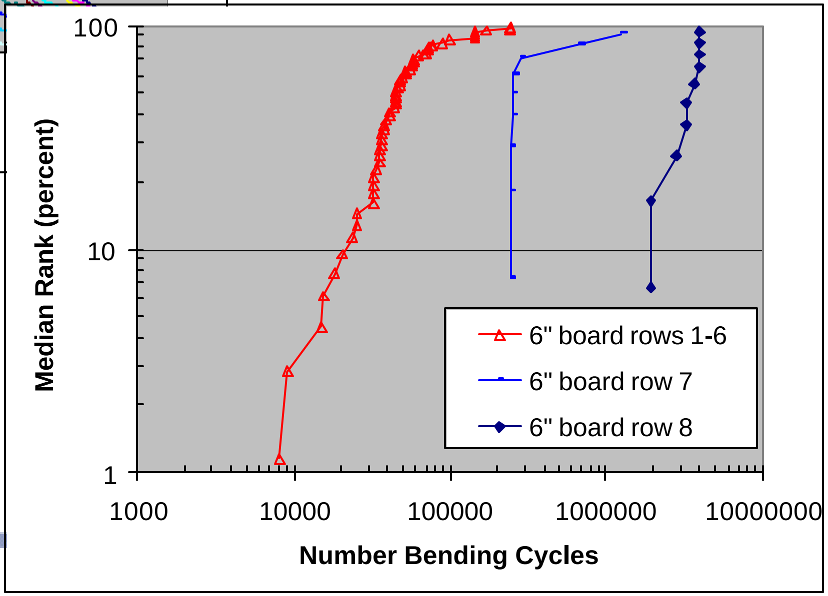

Typical Bend Test Failures

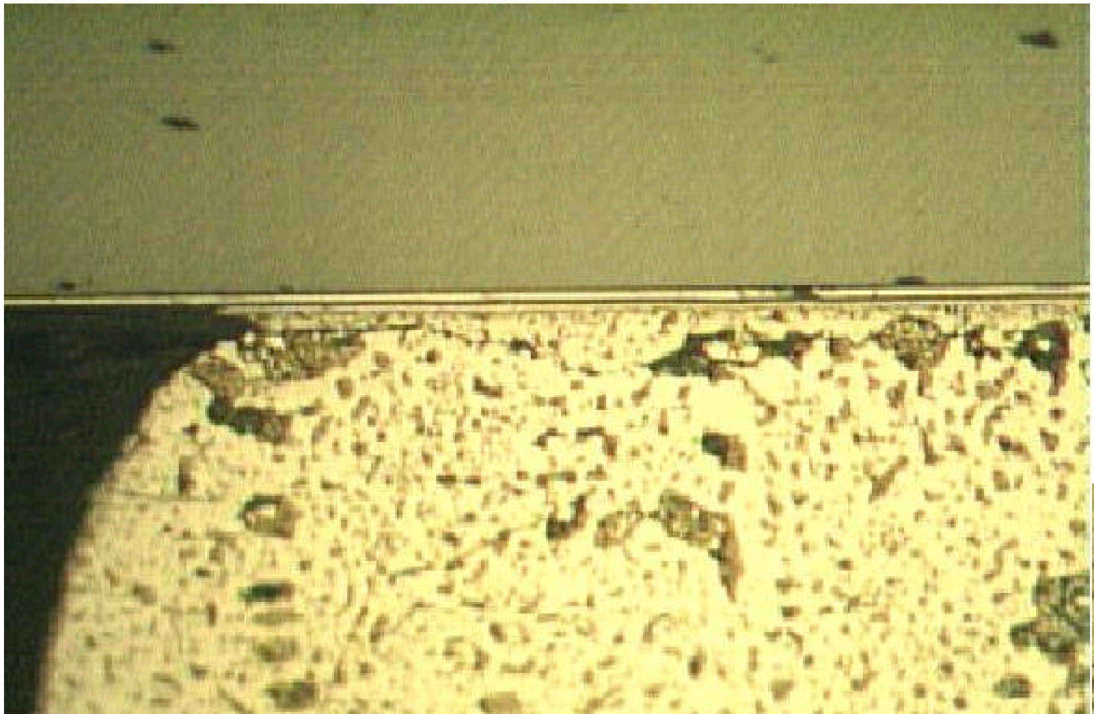

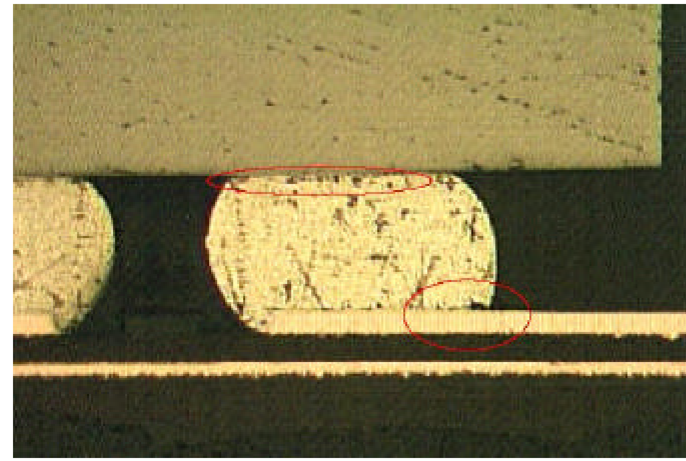

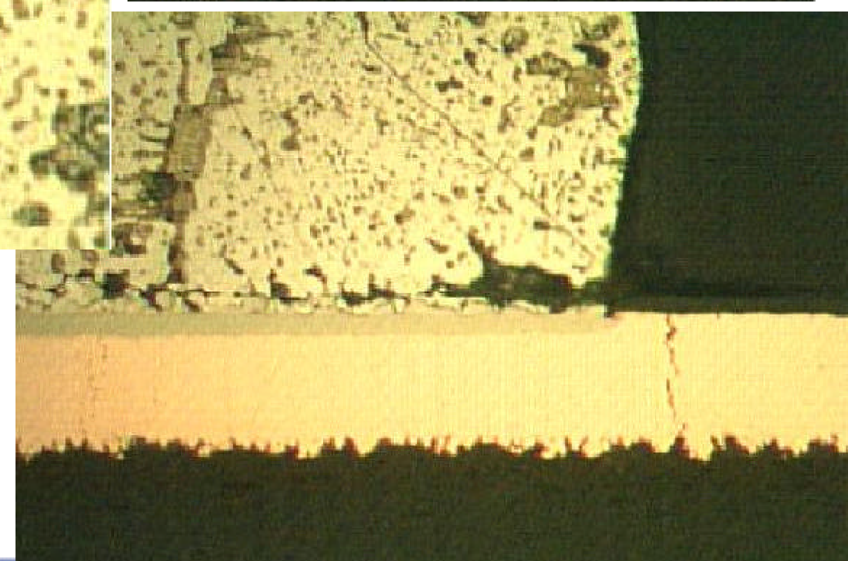

- “Plastic” board response region
  - Board destruction
- Transitional response region
  - Overlap of failure modes
- Elastic board response region
  - Contrasts to temp cycling

Bend Cycling Results

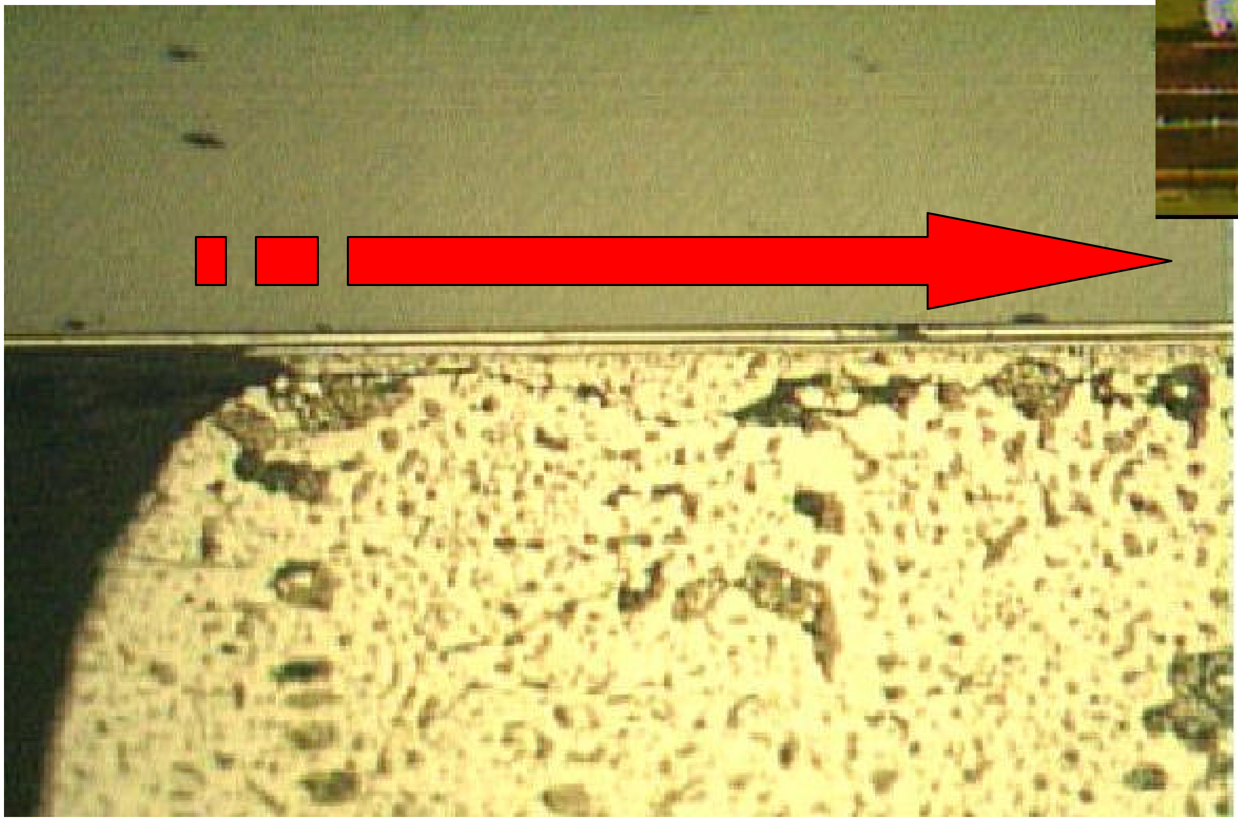

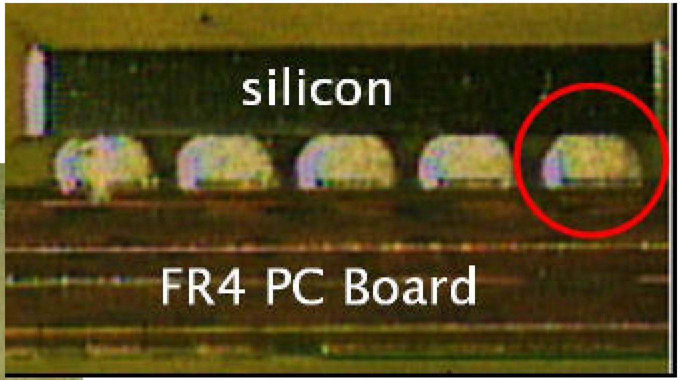

- No domain coarsening
- Crack propagation through solder bump near silicon but…
- Crack begins at “inner” edge and works out

Field Use (Ericsson T39 cell phone)

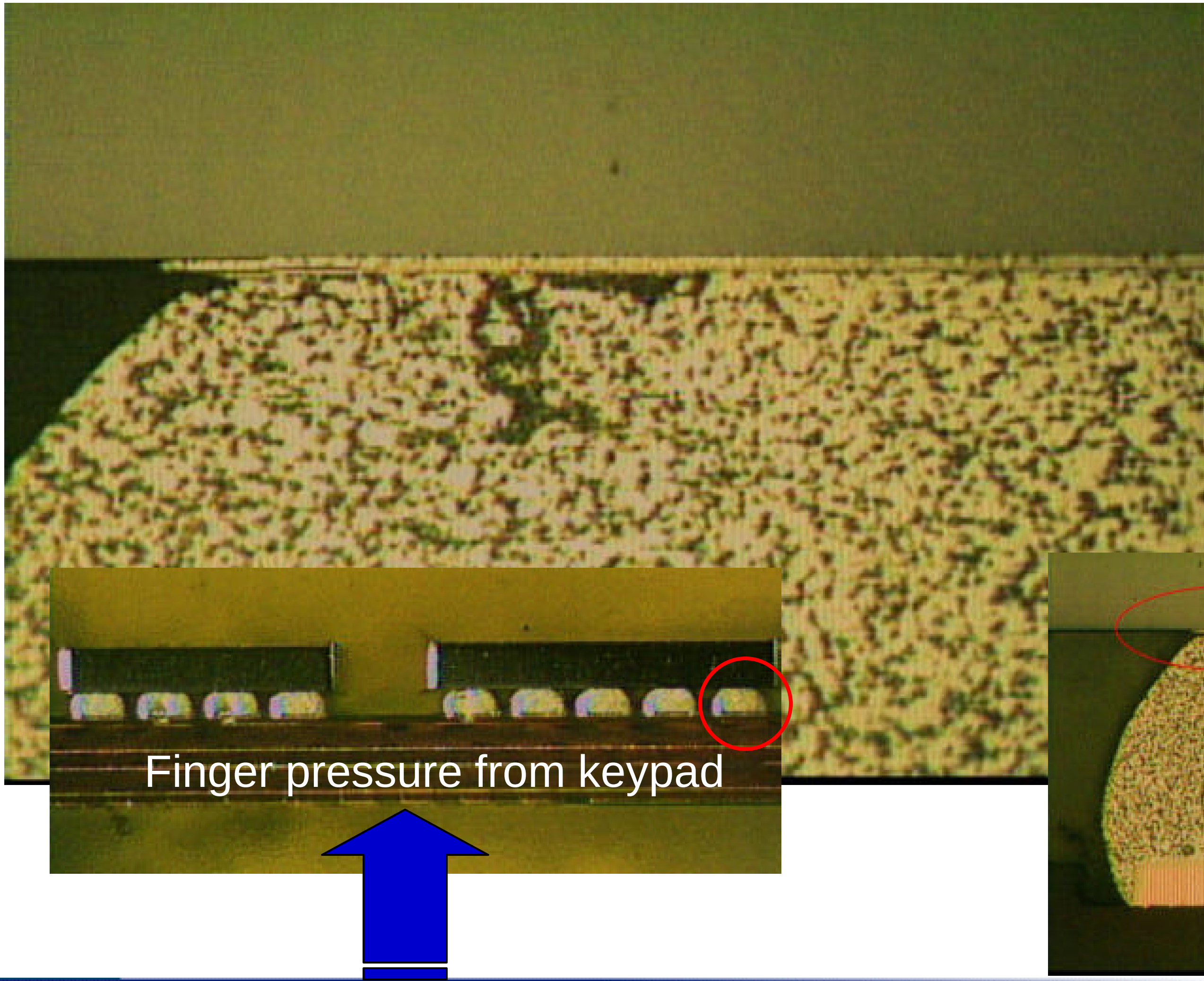

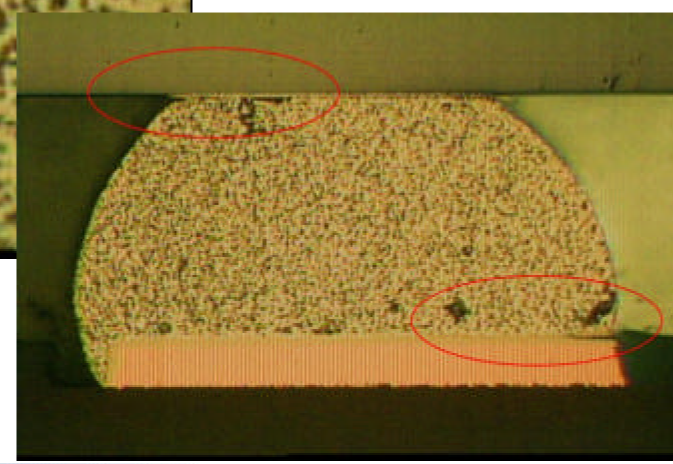

- Relation to bend testing
  - Crack propagation is due to low load cyclic fatigue
  - No domain coarsening
  - Same "wear out" mechanism

Proposed Work

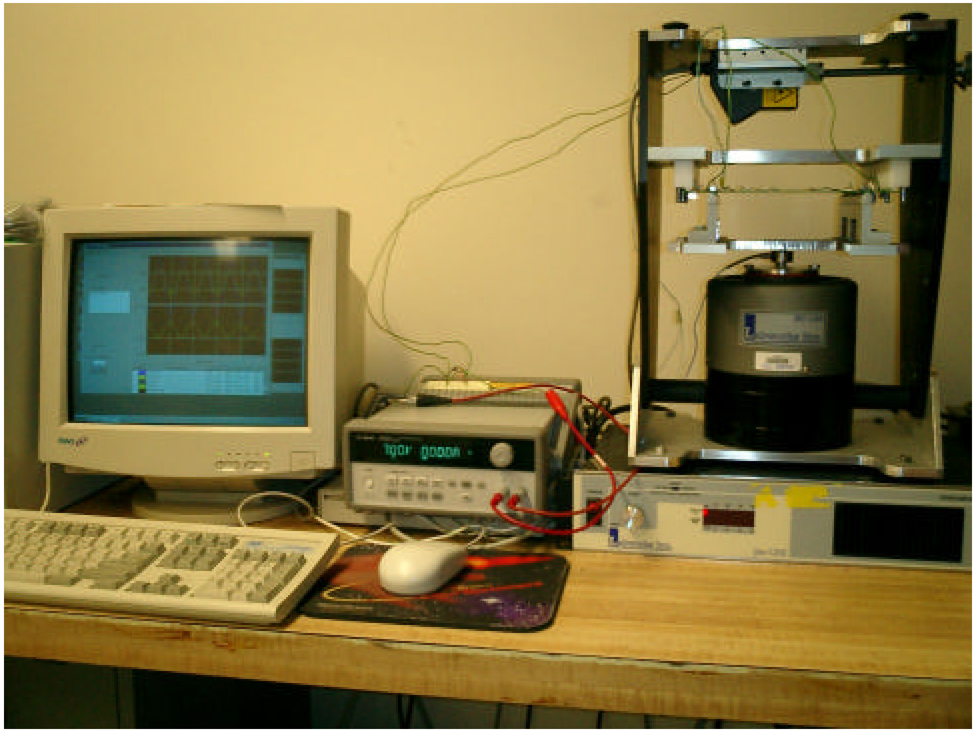

- Multi-Flex Tester
  - Electro dynamic transducer
  - Linear power amplifier
  - Laser optic displacement sensor
  - Multiple waveforms
  - LabWindows/CVI controlled with multiple input and output
  - 5 Hz possible

Fundamental Design

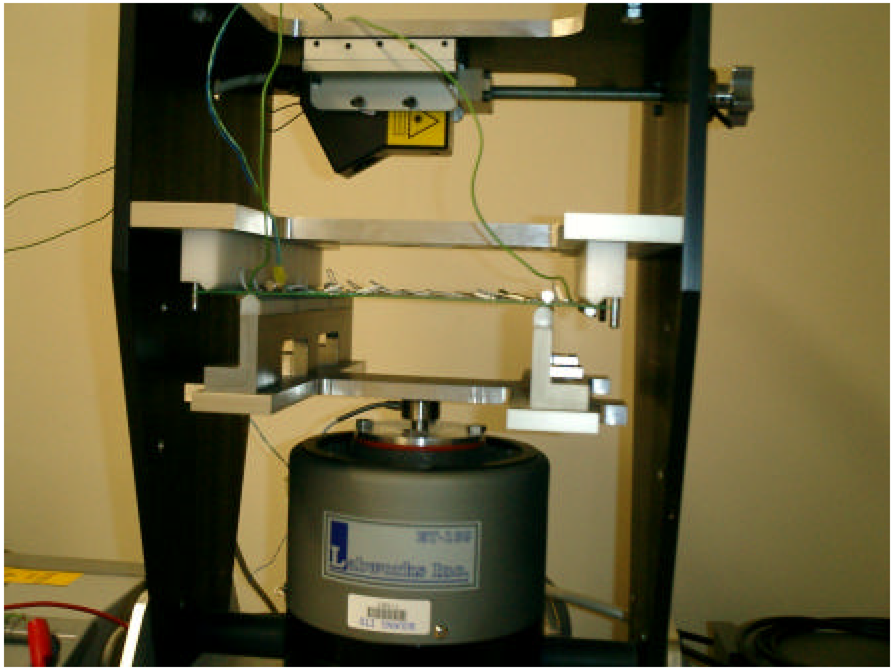

- “4-rod” bend
- Same stress seen on all parts between inner fork (80 parts)
- Magnets create non-friction contact
- Magnets hold board firmly to prevent “slap”

“Optimized” Waveform

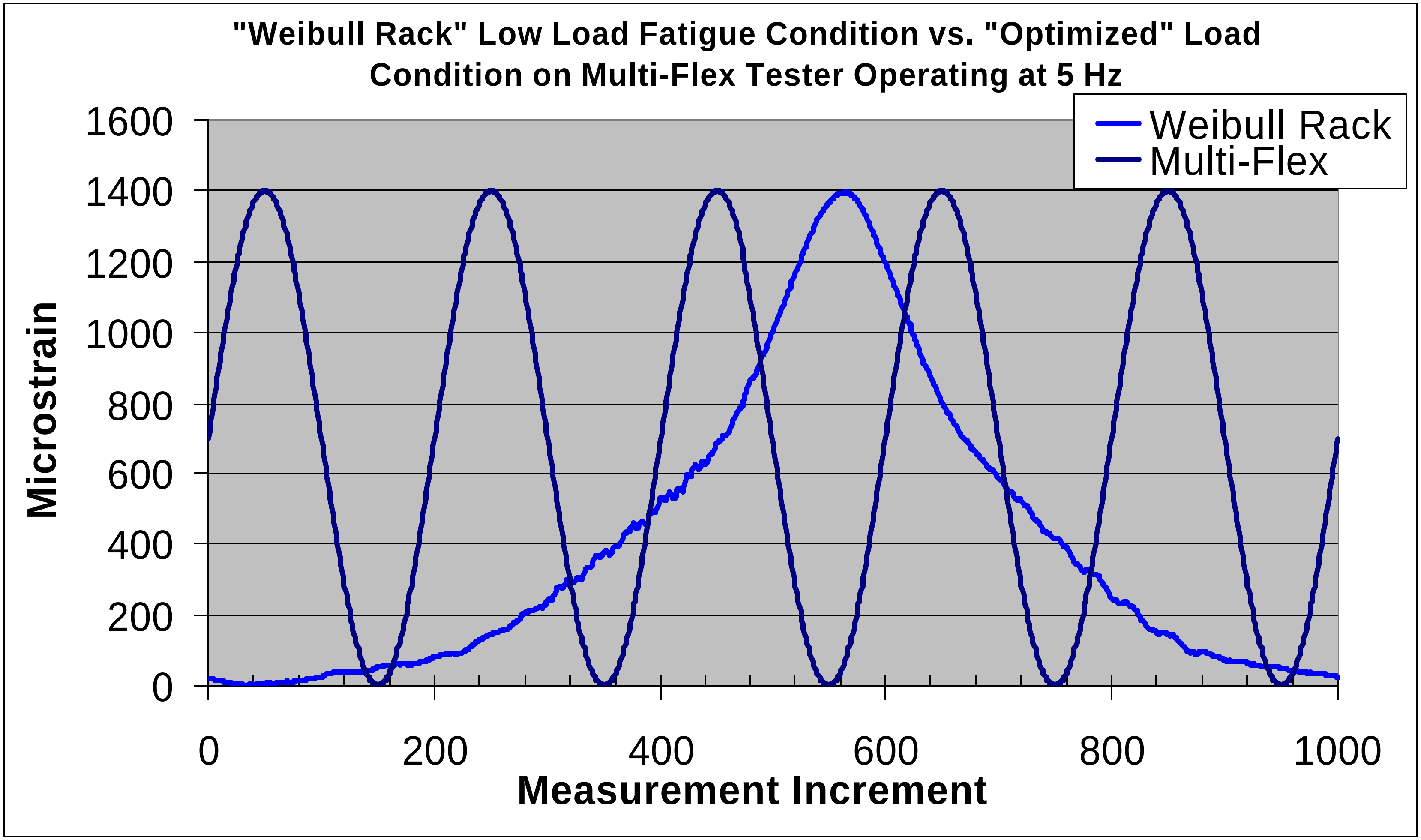

To Do List

- **Near Future**
  - **Characterize Multi-Flex Tester**
  - **Characterize effects of varying silicon thicknesses**
  - **Characterize effects of compliant BCB between bump and silicon**
- **Distant Future**
  - **Construct finite element model**
    - **Compare and contrast computer generated results with both “real world” and experimental results**

Summary

- Temperature Cycling
  - Good for qualification tests
  - Bad for screening tests
  - Slow / Expensive
- Bend Cycling
  - Fast / Inexpensive
  - Applicable to many other hand-held applications
  - Applicable for use with large sample sizes
  - Ideal for screen testing
    - “Weibull Rack”
  - Ideal for CSP qualification testing
    - Multi-Flex Tester

Conclusions

- Bend testing most closely emulates field use
- Therefore, mechanical bend testing is the most accurate and representative testing that can be done for newer hand-held electronic devices
- Testing time and money is drastically reduced with the “Weibull Rack”, as compared to traditional temperature cycling
- Time can be reduced even more with a 5 Hz frequency on the Multi-Flex tester